A&A 413, L5–L9 (2004)
DOI: 10.1051/0004-6361:20034637

Astronomy & Astrophysics

First detection of CO in Uranus

Th. Encrenaz[1], E. Lellouch[1], P. Drossart[1], H. Feuchtgruber[2], G. S. Orton[3], and S. K. Atreya[4]

[1] LESIA, Observatoire de Paris, 92195 Meudon, France
[2] MPI, Postfach 1603, 85740 Garching, Germany
[3] JPL, Pasadena, CA 91109, USA
[4] The University of Michigan, Ann Arbor, MI 48109-1243, USA

Received 30 September 2003 / Accepted 24 November 2003

Abstract. The spectrum of Uranus has been recorded in Oct.–Nov. 2002, between 4.6 and 5.0 μm, using the ISAAC imaging spectrometer at the VLT-UT1 (ANTU) 8-m telescope of ESO. The spectral resolving power was 1500. In addition to a few strong H_3^+ emission lines, the spectrum of Uranus distinctly shows the emission lines of the CO(1–0) band from R7 to P8. The relative intensity distribution of the observed CO emission is not compatible with a thermal distribution, for any value of the rotational temperature. The most likely emission mechanism is fluorescence, and a good fit is obtained assuming a constant CO mixing ratio of 3×10^{-8} at the tropopause and above. The tropospheric continuum of Uranus is also detected beween 4.7 and 5.0 μm. The observed continuum can be fitted assuming reflected sunlight above a cloud level at 3.1 bars, presumably attributed to H_2S. Upper limits of 2×10^{-8} and 1×10^{-6} are inferred for the CO and PH_3 tropospheric mixing ratios above this level. The low CO tropospheric upper limit might suggest that the CO vertical distribution is not uniform.

Key words. planets and satellites: Uranus – infrared: solar system

1. Introduction

In spite of their common status of "icy giants", Uranus and Neptune are known to differ by many aspects. Neptune has a strong energy source while Uranus shows no evidence for it (Gautier & Owen 1989). Neptune's atmosphere exhibits an intense dynamical activity while Uranus is much more sluggish; the eddy diffusion coefficient at the CH_4 homopause is about a few 10^7 cm^2 s^{-1} on Neptune (Romani et al. 1993), while it is less than 10^4 cm^2 s^{-1} on Uranus (Encrenaz et al. 1998). Large abundances of CO and HCN have been detected in Neptune's stratosphere from millimeter and submillimeter spectroscopy, while these species have been so far undetected by this technique in Uranus' atmosphere (Marten et al. 1991, 1993; Rosenqvist et al. 1992). CO, in particular, is about a thousand times more abundant in Neptune's stratosphere (with a mixing ratio of about 10^{-6}) than in Jupiter's troposphere (Bézard et al. 2002), while its stratospheric abundance in Uranus is at least 30 times lower (less than 3×10^{-8}) than the Neptune value. It was suggested by Marten et al. (1993) that convection might be inhibited in some part of Uranus' troposphere, preventing disequilibrium species like CO, HCN or PH_3, to come from the interior.

A good test for this hypothesis would be the detection (or non-detection) of CO and PH_3 in the tropospheres of both Uranus and Neptune. Phosphine, in particular, has been detected in both Jupiter and Saturn, with respective tropospheric P/H ratios of one time and 3−10 times the solar value (Gautier & Owen 1989). Searching for PH_3 in Uranus and Neptune, however, is more difficult than in Jupiter and Saturn, because phosphine, if present in abundances comparable to the solar value, is expected to condense in the upper troposphere, in the vicinity of the 1-bar pressure level. A search for CO and PH_3 on both planets in the submillimeter was unsuccessful, because the penetration level at these wavelengths was restricted to the upper troposphere and above (Encrenaz et al. 1996).

The 5-μm window offers a better opportunity to probe the deep tropospheres of both Uranus and Neptune. As in the case of Jupiter and Saturn, this spectral range is free of methane absorption. According to the atmospheric models of Baines et al. (1995) for Uranus and Neptune, the 5-μm radiation comes from above a cloud deck located at 3.1 bar, presumably made of H_2S ice. The 5-μm window of Uranus was tentatively detected by spectrophotometry by Orton & Kaminski (1989). However, due to the lack of spectral resolution and the limited signal-to-noise ratio, no information could be derived about the atmospheric composition and structure of Uranus.

This Letter presents the first resolved spectrum of Uranus in the 4.6–5.0 μm spectral range. It clearly shows the emission lines of the CO(1–0) band, superimposed over a weak continuum attributed to reflected solar light in the 5-μm tropospheric window. A few strong H_3^+ emission lines are also present. This spectrum provides the first detection of CO in the atmosphere of Uranus.

Send offprint requests to: Th. Encrenaz,
e-mail: Therese.Encrenaz@obspm.fr

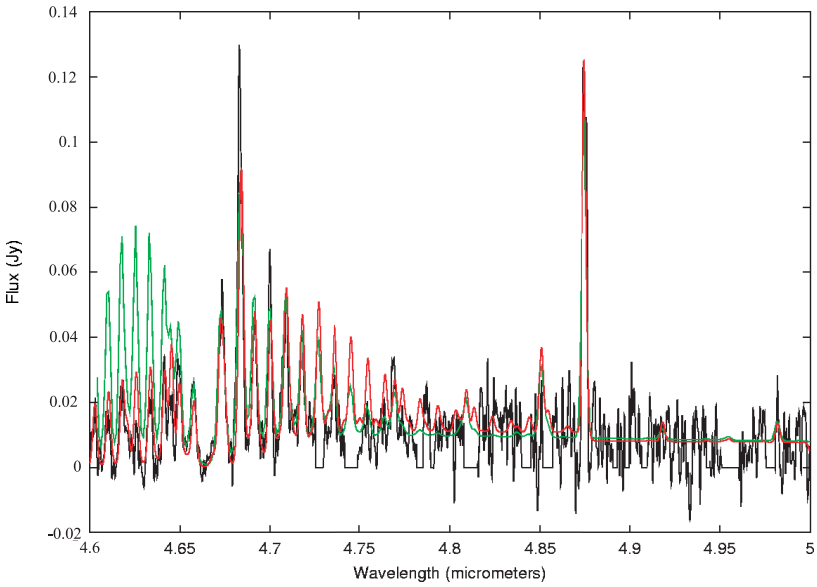

Fig. 1. The calibrated spectrum of Uranus (black line). Red line: best fit model, including CO fluorescence, H_3^+ emission, and tropospheric emission (see text). Green line: three-component model with CO fluorescence replaced by CO thermal emission at 150 K, normalized at 4.71 μm.

2. Observations

Observations were performed in October-November 2002 with the ISAAC (Infrared Spectrometer and Array Camera) instrument mounted on the 8-m VLT-UT1 (ANTU) telescope of the European Southern Observatory at Cerro Paranal (Chile). We used the long-slit spectroscopic mode of the instrument (Cuby et al. 2000), in the long-wavelength mode, which corresponds to a slit height of 120 arcsec and a pixel scale of 0.147 arcsec/pixel; the 1024 × 1024 InSb provides one spectroscopic dimension and one spatial dimension along the slit. The diameter of Uranus was 3.6 arcsec. We used a slit width of 2 arcsec which corresponds to a spectral resolving power of 1500. The standard chopping-nodding procedure along the slit, with a nodding period of 1 min, was used to remove the sky background; this procedure, also used for the observation of Titan at the same wavelength with the same instrument, is fully described in Lellouch et al. (2003). We used two grating positions, covering respectively the 4.60–4.84 μm range (observed on Oct. 15–16, 2002, with a total integration time of 240 min) and the 4.77–5.00 μm range (observed on Nov. 20, 2002, with an integration time of 80 min). The Doppler velocity of Uranus was +24.8 km s^{-1} on October 15–16 and +29.7 km s^{-1} on November 20, which corresponds to a wavelength shift of about 0.00043 μm ($\delta\lambda/\lambda = 10^{-5}$). Although smaller than our spectral resolution, this Doppler shift ensures that the planetary CO lines do not coincide with the telluric lines, and therfore are not absorbed by them.

Data were reduced according with the Eclipse software (Devillard 1997) and the IRAF standard package; a full description of the procedure used can be found in Lellouch et al. (2003). The absolute calibration was achieved using the star HR 8283 (G2V), with a flux of 7.34×10^{-13} W/m^2/μm at 4.80 μm (van der Bliek et al. 1996).

Figure 1 shows the calibrated spectrum between 4.60 and 5.00 μm, obtained from the division of the Uranus raw spectrum by the stellar spectrum. In the region 4.77–4.84 μm where both data sets overlap, we used the data of the first interval (4.60–4.84 μm) which benefited from a longer integration time, and hence a higher signal-to-noise ratio. Data have been replaced by zeros in the spectral regions of very strong telluric absorption. In order to recover the information contained in these spectral ranges, we multiplied, in the modelling phase, the synthetic spectrum of Uranus by a model spectrum of the Earth atmosphere, and the result was convolved to the instrumental function. The telluric absorption model was validated by comparison with the star spectrum.

It can be seen from Figs. 1 and 2 that the observed spectrum of Uranus is the sum of three components. As expected, the spectrum shows a few strong emission lines, especially at 4.684 and 4.875 μm, belonging to the H_3^+ ν_2 fundamental band centered at 4 μm, originating from the upper stratosphere. Other lines of this band have been previously detected (Trafton et al. 1993, 1999; Lam et al. 1997; Encrenaz et al. 2003). Unexpectedly, the spectrum also exhibits a series of emission lines which, as shown in Fig. 1, can all be attributed to the J-components of the CO(1–0) band, between R7 and P8 (4.60–4.73 μm). Two mechanisms can be considered a priori to explain this emission: fluorescence and thermal emission in the stratosphere. Modelling the thermal emission of the CO(1–0) band shows that such a mechanism cannot provide a good fit of the data, especially in the R-branch, for any assumed value of the rotational temperature. This is illustrated in Fig. 1, for $T = 150$ K. This value is about the minimum one which could account for the observed flux level, assuming the lines are optically thick (note that this would imply unrealistically high abundances of CO). For any higher temperature, the discrepancy would be even stronger, as the rotational distribution would extend over larger J-values. We thus exclude a thermal emission mechanism. Finally, the spectrum also shows a weak continuum between 4.75 and 5.00 μm. We attribute this continuum to solar reflection above the cloud level of 3.1 bar presumably due to H_2S ice (Baines et al. 1995). In what follows, we discuss the information obtained from each of the three components.

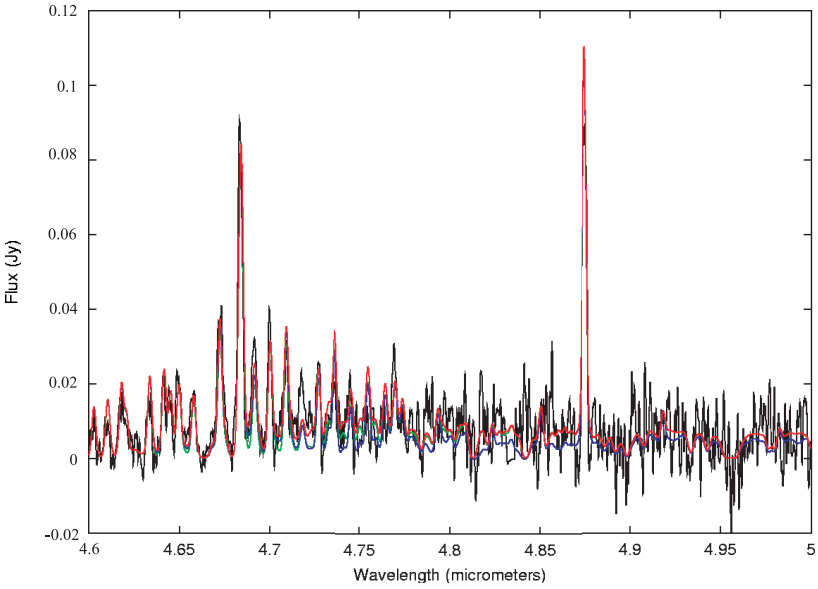

Fig. 2. The raw (undivided) spectrum of Uranus (black line) compared to different synthetic models multiplied by the atmospheric transmission function (see text). Red line: best-fit model (CO = PH_3 = 0); green line: CO = 2.0×10^{-8}, PH_3 = 0; blue line: $PH_3 = 1.0 \times 10^{-6}$, CO = 0.

3. The CO fluorescence

The fluorescence emission of CO in Uranus was calculated using a code derived from the fluorescence model of CH_4 in Jupiter and Saturn, which successfully reproduce the observed methane emission at 3.3 μm in both planets (Drossart et al. 1999). In the case of the CO(1–0) band, we considered the first three energy levels v = 0, 1 and 2. We considered absorption of the solar photons up to levels 1 and 2 followed by radiative and collisional deexcitation down to levels 1 and 0. Direct deexcitation from level 2 to 0 was found to be negligible. We assumed that CO was the only molecule involved in the fluorescence process at n = 2; indeed, CH_4 is condensed in Uranus' stratosphere and its contribution can be considered as negligible.

For each atmospheric level, we performed a radiative transfer non-LTE calculation, including frequency redistribution, along the following steps: (1) full line-by-line calculation of the absorbed solar flux for levels 1 and 2 of CO, at a wavenumber step of 10^{-3} cm^{-1}; (2) calculation of CO vibrational population through detailed balance equations, assuming rotational LTE (the vibrational energy transfer constants are taken from Allen & Simpson (1983), with temperature variations taken into account); (3) line-by-line calculation of spontaneous emission for levels 1 and 2 (using Einstein coefficients from Chandra et al. 1996); (4) calculation of self-absorption of the outgoing flux (which in practice affects only level 1, due to the paucity of level 2 population at Uranus' temperatures); (5) re-injection of the re-absorbed photons in level 1 (resonant scattering), with a Curtis matrix method, adapted to line-by-line calculation. We used the temperature-pressure profile derived from the Voyager 2 radio occultation, adjusted to fit the infrared observations (Griffin & Orton 1993), and we assumed, as a first approximation, a constant mixing ratio of CO.

Calculations show that, because the CO-H_2 collision rate is very weak, the coefficient $\epsilon = \nu_{coll}/\nu_{rad}$ (ν_{coll} and ν_{rad} being the collisional rate and the spontaneous emission rate respectively) which is inversely correlated to the fluorescence efficiency (Appleby 1990), is very low, as compared to the case of CH_4. As a result, non-LTE effects (measured by the parameter $\chi = 1/(1+\epsilon)$) start to play a role at relatively low altitudes, around the tropopause (χ = 0.1 at P = 100 mbar), and become predominent (χ larger than 0.6) above the 10 mb-level. This situation is very different from the case of the methane fluorescence in the giant planets (Drossart et al. 1999), because the CO-H_2 collision rate is about 100 times smaller than the CH_4-H_2 rate. A good fit of the observed CO emission in Uranus is achieved for a mean CO mixing ratio of 3.0×10^{-8} (Figs. 1 and 2). Another result of our calculation is that the (2–1) emission band intensity is expected to be about ten percent of the (1–0) band one; this is consistent with our data, where the CO(2–1) band is undetected.

Because the CO fluorescence partly originates at depth, a complete fluorescence model might have to take into account scattering effects by cloud particles. This is a very unusual case for non-LTE radiative transfer which would add still more complexity to the model, and has not been taken into account. The effect of scattering would be to increase the photon atmospheric path, and thus decrease the vertical CO column density needed to fit the data. Our mixing ratio could then be overestimated. All the uncertainties of the model make the CO estimated abundance probably uncertain by at least a factor of 2.

4. The tropospheric model

The 5-μm window in Uranus is dominated by the ν_2 fundamental band of CH_3D centered at 4.54 μm which limits the blue side, and the collision-induced absorption (CIA) of hydrogen on the red side. The CIA contribution, calculated from Birnbaum et al. (1996) was found to be negligible below 5 μm. Water and ammonia absorptions are found to be negligible in the spectrum of Uranus, as these species condense below the tropospheric levels probed at 5 μm.

The temperature profile of Griffin & Orton (1993) was used, down to the H_2S cloud level at 3.1 bar (Baines et al. 1995). The thermal component is found to be negligible (for T = 120 K, the emitted blackbody flux is only 0.003 Jy at

5 μm). The incident solar radiance is taken from Vernazza et al. (1976). We assumed a tropospheric mixing ratio of 2.3×10^{-2} for CH_4 (West et al. 1991) and a D/H ratio of 5×10^{-5} (Feuchtgruber et al. 1999). Saturation of CH_4, CH_3D and PH_3 was included in our calculations. Methane condensation occurs at 75 K (P = 1 bar) for CH_4, and also for PH_3 when the PH_3 mixing ratio is assumed to be 2×10^{-6}. Spectroscopic parameters were taken from the HITRAN data base.

It can be seen from Fig. 2 that the best fit is achieved when neither CO nor PH_3 are present. The fit is still not satisfactory at some wavelengths, especially in the vicinity of strong telluric absorptions; however, adding CO and/or PH_3 absorptions tends to degrade the fit over the whole spectral range. We derive from Fig. 3 upper limits of 2×10^{-8} and 1×10^{-6} for tropospheric CO and PH_3 respectively. These values are more constraining than those derived in the submillimeter range (5×10^{-7} and 2×10^{-6} for CO and PH_3 respectively; Encrenaz et al. 1996).

As shown in Figs. 1 and 2, our tropospheric model without any CO and PH_3 absorption provides an overall satisfactory fit to the data, which validates the model we used with a reflection above the P = 3.1 bar level. This model was also successful for modelling the 2.7 μm window of Uranus as observed with the ISO spectrophotometer PHT-S (Encrenaz et al. 2000). From the ISO data we derived a very low albedo (0.006) for the cloud level (presumably made of H_2S) at 2.7 μm. From the ISAAC-VLT data, we infer at 5 μm an albedo of 0.0036, nearly half of the 2.7 μm value. As mentioned in our previous study, we have no explanation for this very low value.

5. The H_3^+ emission

Several H_3^+ emission lines are shown in our Uranus spectrum (Figs. 1 and 2). The two strongest lines appear at 4.684 and 4.875 μm. Other strong transitions are present at 4.645 and 4.659 μm, and weaker lines appear at 4.770 and 4.809 μm. In principle, the rotational temperature could be retrieved from the relative intensities of the two strongest lines; unfortunately, the 4.684 μm line is blended with the CO fluorescence emission, as are the weaker H_3^+ lines. In addition, we note that the intensity ratio of the two strongest lines at 4.875 and 4.684 μm varies by 13 percent only when T varies from 500 to 700 K. Because of the CO fluorescence contribution in the H_3^+ line at 4.684 μm, we cannot determine the H_3^+ rotational temperature. Recent measurements of the H_3^+ infrared emission around 4 μm led to estimates of 560 ± 40 K and 640 ± 40 K in September 2000 and September 2001 respectively (Encrenaz et al. 2003). Assuming a rotational temperature of 600 K for the VLT data, we infer an H_3^+ column density of 9×10^{11} cm^{-2}. The uncertainty on this result is large, due to the uncertainty on the rotational temperature: assuming temperatures of 500 K and 700 K, the H_3^+ column density would become 25×10^{11} and 5×10^{11} cm^{-2} respectively. Our mean estimate is higher than the values inferred in 2000 and 2001 ($5.1(^{+3.2}_{-1.4}) \times 10^{11}$ cm^{-2} and $4.0(^{+1.8}_{-1.0}) \times 10^{11}$ cm^{-2} respectively), but still within the range of interannual variations. The 2003 result is still consistent with the general trend of the H_3^+ emission, which appears to be globally in phase with the solar activity (Trafton et al. 1999).

6. Discussion

Our data bring the first evidence for the presence of CO in the atmosphere of Uranus. On one hand, our fluorescence observations are consistent (within an uncertainty factor of at least 2) with a mean CO mixing ratio of 3×10^{-8} above a level approximately located at 0.1 bar. On the other hand, our tropospheric model rules out a mean CO tropospheric mixing ratio higher than 2×10^{-8} above the 3.1-bar level. A third constraint is provided by the millimeter upper limit of 3×10^{-8} which refers to the middle stratosphere, probably above the 10-mbar level (Marten et al. 1993). The large uncertainty of the CO abundance derived from the fluorescence spectrum prevents us to derive firm conclusions about the CO vertical distribution. A dynamical modelling taking into account the eddy diffusion coefficient, combined with vertically inhomogeneous fluorescence models including possible scattering effects, will be needed for this purpose. However, if the numbers given above were confirmed, the combination of the three constraints would imply that the CO mixing ratio in Uranus cannot be constant throughout the atmosphere, but would have to be depleted below the tropopause. If CO were of internal origin, we would expect its mixing ratio to be constant up to the homopause, at about 1 mbar (Encrenaz et al. 1998). We would thus have to conclude that CO is likely to be mostly of external origin. As in the case of external H_2O (Feuchtgruber et al. 1997), the CO source could come from icy satellites and/or interplanetary meteorites. Finally, we should mention that lightning in Uranus (Zarka & Pedersen 1986) could also be considered as a third possible source of CO (Podolak & Bar-Nun 1988); however, this process would be expected to take place at lower altitudes, in the vicinity of the H_2O cloud.

The upper limits retrieved for the tropospheric mixing ratios of CO and PH_3 suggest that, as proposed by Marten et al. (1993), convection might be locally inhibited in Uranus' upper troposphere, leading to the absence of disequilibrium species and the lack of dynamical activity. The origin of this inhibition, probably connected to the absence of internal heat, would remain to be understood.

Acknowledgements. The authors were visiting astronomers at the VLT, European Southern Observatory (Program 70.C-0062A). We thank the ESO staff members for their help and support.

References

Allen, D. C., & Simpson, J. S. M. 1983, Chem. Phys., 76, 231
Appleby, J. F. 1990, Icarus, 85, 355
Baines, K. H., Mickelson, M. E., Larson, Lee, E., & Ferguson, D. W. 1995, Icarus, 114, 328
Bézard, B., Lellouch, E., Strobel, D., Maillard, J.-P., & Drossart, P. 2002, Icarus, 159, 95
Birnbaum, G., Borysow, A., & Orton, G. S. 1996, Icarus, 123, 4
Chandra, S., Melshwari, V. U., & Sharma, A. J. 1996, A&AS, 117, 557
Cuby, J.-G., Lidman, C., & Moutou, C. 2000, The Messenger, 101, 2
Devillard, C. 1997, The Messenger, 87
Drossart, P., Fouchet, T., Crovisier, J., et al. 1999, ESA SP-427, 169
Encrenaz, Th., Serabyn, E., & Weisstein, E. W. 1996, Icarus, 124, 616

Encrenaz, Th., Feuchtgruber, H., Atreya, S. K., et al. 1998, A&A, 333, L43
Encrenaz, Th., Schulz, B., Drossart, P., et al. 2000, A&A, 362, 1174
Encrenaz, Th., Drossart, P., Orton, G. S., et al. 2003, Plan. Space Sci., in press
Feuchtgruber, H., Lellouch, E., de Graauw, T., et al. 1997, Nature, 389, 159
Feuchtgruber, H., et al. 1999, A&A, 341, L17
Gautier, D., & Owen, T. 1989, The composition of outer planet atmospheres, in Origin and evolution of planetary and satellite atmospheres, ed. S. K. Atreya, J. B. Pollack, & M. S. Matthews (University of Arizona Press), 487
Griffin, M. J., & Orton, G. S. 1993, Icarus, 105, 537
Lam, H. A., Miller, S., Joseph, R. D., et al. 1997, ApJ, 474, L73
Lellouch, E., Coustenis, A., Sebag, B., et al. 2003, Icarus, 162, 125
Marten, A., Gautier, D., Owen, T., Sanders, D., et al. 1991, Bull. Am. Astron. Soc., 23, 1164
Marten, A., Gautier, D., Owen, T., Sanders, D. B., et al. 1993, ApJ, 406, 285
Orton, G. S., & Kaminski, C. D. 1989, Icarus, 77, 109
Podolak, M., & Bar-Nun, A. 1988, Icarus, 75, 566
Romani, P., Bishop, J., Bézard, B., & Atreya, S. K. 1993, Icarus, 106, 442
Rosenqvist, J., Lellouch, E., Romani, P. N., Paubert, G., & Encrenaz, T. 1992, ApJ, 392, L99
Trafton, L. M., Geballe, T. R., Miller, S., Tennyson, J., & Ballester, G. E. 1993, ApJ, 405, 761
Trafton, L. M., Miller, S., Geballe, T. R., Tennyson, J., & Ballester, G. E. 1999, ApJ, 524, 1059
van der Bliek, N. S., Manfroid, J., & Bouchet, P. 1996, A&AS, 119, 547
Vernazza, J. E., Avrett, E. H., & Loeser, R. 1976, ApJS, 30, 1
West, R. A., Baines, K. H., & Pollack, J. B. 1991, Cloud and aerosols in the Uranus atmosphere, in Uranus, ed. J. T. Bergstralh, E. D. Miner, & M. S. Matthews (University of Arizona Press), 296
Zarka, P., & Pedersen, B. 1986, Nature, 323, 605